Study of stress relief and strain distribution in graphene films of biosensors for viral infections

© I.A. Eliseyev[1], A.S. Usikov[1,2], A.D. Roenkov[2], S.P. Lebedev[1], V.N. Petrov[1], A.N. Smirnov[1], A.A. Lebedev[1], E.V. Gushchina[1], E.M. Tanklevskaya[1], E.I. Shabunina[1], M.V. Puzyk[3], N.M. Schmidt[1]

[1] Ioffe Institute,
St. Petersburg, Russia
[2] Nitride Crystals Group,
St. Petersburg, Russia
[3] Herzen State Pedagogical University of Russia,
St. Petersburg, Russia

E-mail: ilya.eliseyev@mail.ioffe.ru

Received May 19, 2023
Revised September 25, 2023
Accepted October 30, 2023

The practical application of graphene-based biosensors for viral infections is largely hampered by the irreproducibility of their parameters, including the adsorption properties of graphene in biosensors. In this work, a new source of irreproducibility of biosensor parameters caused by the formation of a stress relief on the graphene surface was experimentally discovered. Monitoring the topography of the graphene surface using atomic force microscopy together with analysis of graphene deformation using Raman spectroscopy makes it possible to reject plates with stress relief and significantly increase the reproducibility of biosensor parameters.

Keywords: graphene, biosensors, Raman spectroscopy, atomic force microscopy.

DOI: 10.61011/PSS.2023.12.57683.5197k

Due to their extraordinary sensitivity the graphene-based biosensors are promising for use in medicine and biology. The use of graphene films to create biosensors, including viral infections, showed that the adsorption properties of graphene in biosensor chips can deteriorate compared to the original graphene film [1,2]. The properties deterioration is observed at the initial stage of topology formation of biosensor chips using photolithography (PLG) methods. Numerous studies [2,3] have shown that during PLG the interaction of photoresist with graphene occurs, with the formation of local areas with resist residues (LRR). The graphene surface roughness increases as a result. The issue is exacerbated by the fact that the traditional optical microscopic technique used to verify the removal of a photoresist is insensitive to LRRs. Atomic force microscopy (AFM) and Raman scattering spectroscopy (RSS) provide the most comprehensive data on LRRs [4,5]. Our previous studies showed that the presence of LRR on the biosensor graphene leads to a non-uniform distribution of deformations [5]. As a result, the scattering in the resistance values of biosensor chips obtained from one wafer increases, and the efficiency of virus detection decreases, up to the value where the biosensor signal does not depend on the concentration of viruses [5]. The low reproducibility of biosensor chip parameters, noted in many publications [2,6], prevents the widespread use of graphene-based biosensors in the viral infections control.

Deformation is an effective way to control the electronic properties of two-dimensional materials [6] due to their excellent elasticity and high Young's modulus, in contrast to bulk materials. The influence of the local stress relief of graphene in biosensor chips on the reproducibility of parameters and the detection properties of the chips practically was not studied.

Two-dimensional materials, including graphene, are characterized by a special type of local deformation — the formation of a wavy relief, also called a stress relief [1,3], which in the general case is a means of partial relaxation of excess stresses. The waves can cause symmetry breaking, as well as the occurrence of structural disorder in graphene, which, in turn, leads to the formation of clusters of electrons and holes and, thus, to spatial inhomogeneity in the distribution of charge carriers.

This paper contains the results of studying wafers and chips with stress relief using AFM and RSS methods. Recommendations are given for improving the reproducibility of the parameters of biosensor chips made from graphene on SiC.

The studies were carried out on chips with two ohmic contacts mounted on textolite holder. Size of sensor area is $1 \times 1.5\,\text{mm}^2$. Chips were fabricated from several wafers with graphene films formed by thermal decomposition of semi-insulating substrates 4*H*-SiC. Details of the technology for graphene films formation and the main stages of biosensors creation are described in papers [4,5]. The study of graphene films on wafer and in chips by AFM methods was carried out on Ntegra AURA unit (NT-MDT, Russia) using a HA_FM cantilever (www.tipsnano.com), with a radius of curvature of less than 10 nm. The scanning field size was 256×256 points. The current-voltage curves (CVC) of graphene in the chips were measured on KEITHLEY 6487 unit. RSS spectra were measured at room temperature in

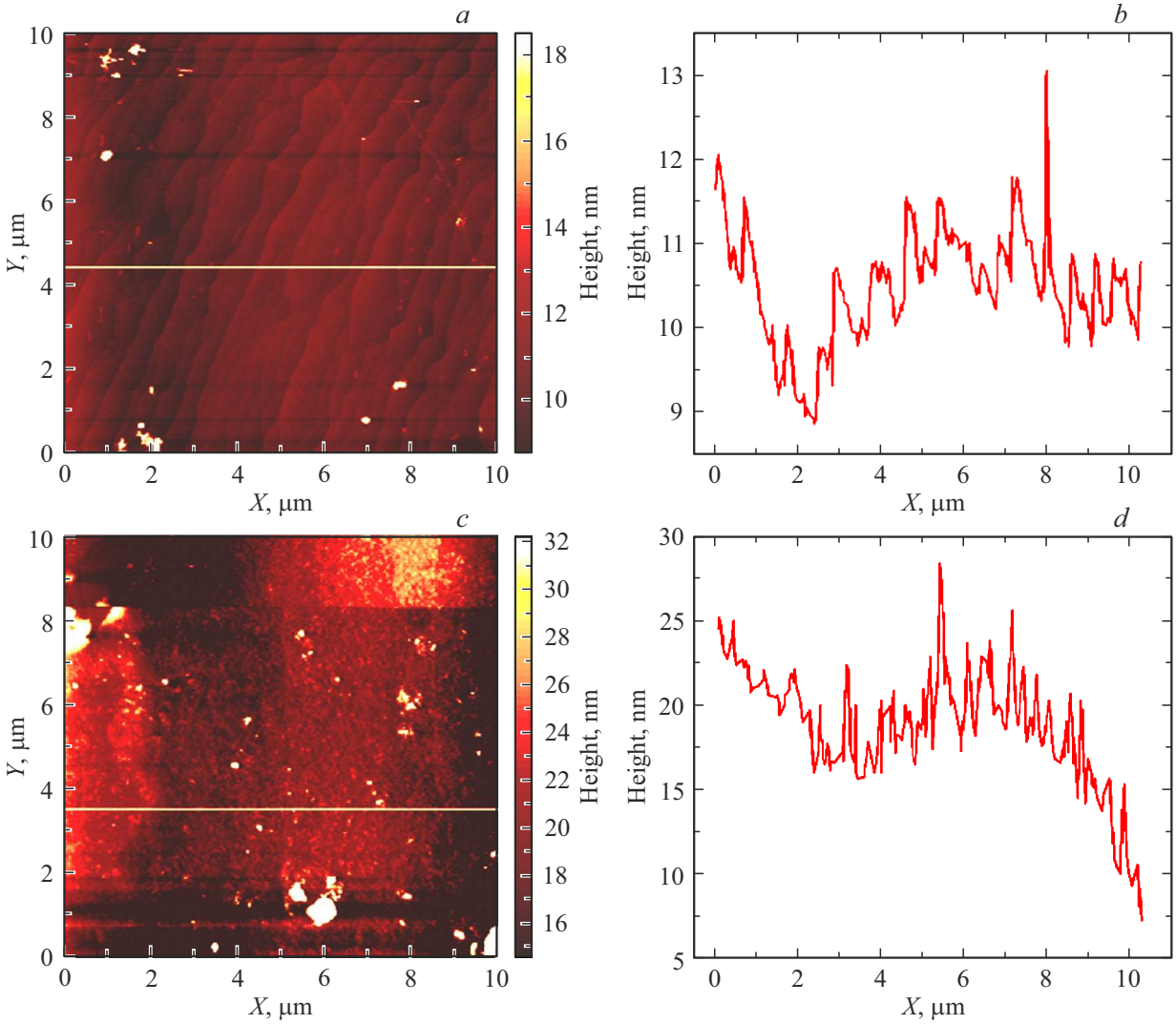

Figure 1. AFM images of surface topography and graphene roughness profiles (measured along a horizontal line in AFM images) in chip areas: *a, b* — with local stress relief, *c, d* — with local stress relief, reinforced by resist residues.

the backscattering geometry with Horiba LabRAM HREvo UV-VIS-NIR-Open spectrometer fitted with a confocal microscope with lens Olympus MPLN100 × (NA = 0.9). The power of the YAG : Nd laser with wavelength of 532 nm was 4.0 mW in a spot with a diameter of 1 μm. Along with local measurements, sample regions of size $10 \times 10\,\mu m^2$ were analyzed with subsequent plotting of maps of the distribution of spectral line parameters.

AFM studies of graphene in chips after PLG with monitoring of resist removal with optical microscope revealed inhomogeneously distributed regions with LRR, leading to increase in the RMS roughness values of the graphene surface from by 2 to 10 times relative to the values in the graphene film before PLG — 0.4 nm. At the same time, RSS data indicate inhomogeneous distribution of compressive deformations from 0.2 to 0.6%. As a result, there is scattering in the graphene resistance values in chips from 1–10 kOhm. Detailed experimental data are given in our previous paper [6]. The introduction of the procedure for additional washing of LRR identified by AFM methods made it possible to obtain in graphene on some of the chips RMS roughness of 0.4–0.5 nm, close to the values on the graphene film before pLG. At the same time, the scattering of graphene resistance values in the chips decreased to 1 –1.3 kOhm.

However, on some of the chips of individual wafers, in the images of graphene topography in the field $10 \times 10\,\mu m^2$, areas with stress relief were identified (Figure 1, *a*). The formation of the relief is identified in the roughness profiles of the graphene surface. An example of the roughness profile with a occurred stress relief is shown in Figure 1, *b*. The period of alternation of relief humps is about 5 μm, and their amplitude is about 2 nm. In this case, the RMS roughness increases to 4 nm. As a rule, chips with graphene with the stress relief had a resistance over 2 kOhm. Note that this relief is not present over the entire area of the chip.

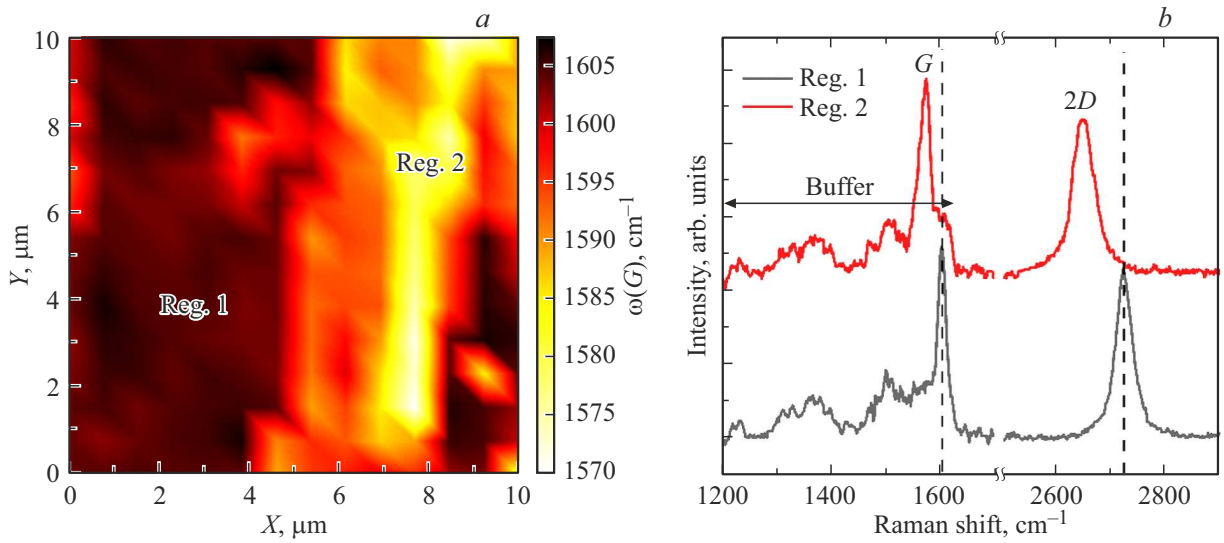

Figure 2. RSS map of line frequency distribution G (a) and typical RSS spectra obtained in regions 1 and 2 (b).

When studying graphene, local regions without stress relief were discovered, in them there was exclusively a step relief characteristic of graphene grown on SiC [7], and the RMS roughness was 0.5 nm.

Figure 1, c, d shows the map and profile of the surface topography for the same chip in the area with LRR. It is clearly seen that against the background of the general picture of contamination associated with resist residues, an envelope is observed in the surface topography profile, the amplitude of the envelope is by several times higher than the amplitude of the relief in Figure 1, b. The presence of resist residues precisely in areas with a stress relief supposes increase in the interaction of the resist with graphene in such areas.

Graphene in biosensor chips was also studied in several areas using RSS mapping. Based on the results of these studies the distribution maps of various parameters of spectral lines of graphene were plotted: G and $2D$, in particular their frequencies. It is known that compressive deformation leads to a shift of the G line towards high frequencies, and tensile deformation leads to the shift towards low frequencies relative to its position in undeformed graphene. In addition, the presence of a selected deformation axis leads to the removal of degeneracy and splitting of the line G [8], which at small values of deformation can manifest itself in the form of its broadening.

Figure 2 shows RSS mapping data obtained in the area of the chip, which is characterized by stress relief. On the frequency distribution map of the line G (Figure 2, a), two characteristic areas are distinguished: with a frequency in the range $1595-1607\,\mathrm{cm}^{-1}$ (region 1) and with frequency in the range of $1565-1590\,\mathrm{cm}^{-1}$ (region 2). Typical spectra for each region are presented in Figure 2, b. In both spectra, features characteristic of high-quality monolayer graphene grown on 4H-SiC substrate are observed: G- and $2D$-lines, as well as the contribution of the buffer layer [7]. The line D ($\sim 1350\,\mathrm{cm}^{-1}$), prohibited by the selection rules in defect-free graphene, is absent in the spectra, which confirms the high structural perfection of the graphene film.

Lines G ($1603\,\mathrm{cm}^{-1}$) and $2D$ ($2722\,\mathrm{cm}^{-1}$) in the spectrum from region 1 are shifted towards high frequencies relative to their position in undeformed graphene on SiC substrate (1581 and $2691\,\mathrm{cm}^{-1}$, respectively [9]), which is characteristic of most graphene samples on SiC and is associated with the presence of biaxial compressive deformation, the magnitude of which is of the order of -0.3% [9]. In the spectrum from region 2 the frequency of the lines G and $2D$ is significantly lower (1574 and $2650\,\mathrm{cm}^{-1}$, respectively) than in undeformed graphene. Besides, the full width at half maximum (FWHM) of the line G at point 2 is $25\,\mathrm{cm}^{-1}$, and the line $2D$ — $43\,\mathrm{cm}^{-1}$, which is by $10\,\mathrm{cm}^{-1}$ higher than the value of these parameters at point 1.

The position of the RSS spectrum lines of graphene depends on many factors, the most significant of which are deformation, charge carrier concentration, and the Fermi velocity of electrons in graphene. The influence of each of these factors on the position of the lines G and $2D$ is different; a more detailed analysis of them is presented in the paper [9] and the papers cited therein. Since simultaneous consideration of all three factors is significantly difficult, and the question of the possible influence of LRR on the Fermi rate is a topic for a separate paper, one factor whose influence is most pronounced was chosen for analysis. In the case of RSS spectrum from region 2, such factor is deformation, since the shift of the lines G and $2D$ towards low frequencies, simultaneously with their broadening, is characteristic of the occurrence of uniaxial tensile deformation in graphene. Its value, estimated from the shift of the line $2D$, is 0.36% [8]. Note that the increase in FWHM lines G and $2D$ can also be contributed by the presence of defects in the graphene crystal lattice [10],

although their concentration, based on the absence of line contribution D against the background of the spectrum of the buffer layer should be small.

Thus, analysis of RSS data indicates the presence of compression (region 1) and tension (region 2) regions in the graphene film. Due to the fact that the distance between the centers of the regions with decreased and increased deformation values corresponds to the period of the local relief, we can assume that this deformation pattern, which is uncharacteristic of graphene on SiC, is associated precisely with the presence of a stress relief. The presence of deformed regions of tension and compression can lead to the existence in these regions of clusters of antipodes-defects, including those with opposite charges. As a result, the transport of charge carriers occurs along flow channels and is accompanied by an increase in the graphene resistance in the chip. On some chips, in regions of stress relief the interaction of the resist with graphene increases (Figure 1, *c, d*). As a result, resist residues removal becomes impossible even through additional washing, which leads not only to increase in the chip resistance, but also to deterioration in the adsorption properties of graphene in the chips. Monitoring of the wafers topography before PLG using AFM methods makes it possible to reject wafers with graphene that have stress relief and increase the reproducibility of parameters of biosensor chips, as well as adjust the technological regimes of graphene formation.

Thus, the presence of regions with a local stress relief worsens the reproducibility of graphene parameters in chips. It was found that the stress relief appears even before PLG, during the graphene film formation on silicon carbide. It was demonstrated that the appearance of this relief is accompanied by the appearance of regions uncharacteristic of graphene on SiC with alternating compressive and tensile deformation. The topography monitoring of the graphene film on SiC before PLG makes it possible to identify plates with a local stress relief, to eliminate their use in the production of biosensor chips, and thus to increase significantly the reproducibility of biosensor parameters.

Funding

A.S. Usikov, A.N. Smirnov and E.V. Gushchina thank the Russian Science Foundation for their support (project No. 22-12-00134 https://rscf.ru/project/22- 12-00134/).

Conflict of interest

The authors declare that they have no conflict of interest.

References

[1] D.M. Mackenzie, J.D. Buron, P.R. Whelan, J.M. Caridad, M. Bjergfelt, B. Luo, A. Shivayogimath, A.L. Smitshuysen, J.D. Thomsen, T.J. Booth, L. Gammelgaard, J. Zultak, B.S. Jessen, P. Bøggild, D.H. Petersen. Nano Res. **10**, 3596 (2017).

[2] I. Shtepliuk, F. Giannazzo, R. Yakimova. Appl. Sci. **11**, *13*, 5784 (2021).

[3] A. Choi, A.T. Hoang, T.T. Ngoc Van, B. Shong, L. Hu, K.Y. Thai, J.-H. Ahn. Chem. Eng. J. **429**, 132504 (2022).

[4] N.M. Shmidt, A.S. Usikov, E.I. Shabunina, A.V. Naschekin, E.V. Gushchina, I.A. Eliseyev, V.N. Petrov, M.V. Puzyk, O.V. Avdeev, S.A. Klotchenko, S.P. Lebedev, E.M. Tanklevskaya, Yu.N. Makarov, A.A. Lebedev, A.V. Vasin. Biosensors **12**, *1*, 8 (2022).

[5] I.A. Eliseev, E.A. Gushchina, S.A. Klotchenko, A.A. Lebedev, N.M. Lebedeva, S.P. Lebedev, A.V. Nashchekin, V.N. Petrov, M.V. Puzyk, A.D. Roenkov, A.N. Smirnov, E.M. Tanklevskaya, A.S. Usikov, E.I. Shabunina, N.M. Schmidt. FTP **56**, *12*, 1137 (2022). (in Russian).

[6] X. Li, L. Tao, Z. Chen, H. Fang, X. Li, X. Wang, J.-B. Xu, H. Zhu. Appl. Phys. Rev. **4**, *2*, 021306 (2017).

[7] A.A. Lebedev, V.Yu. Davydov, D.Yu. Usachov, S.P. Lebedev, A.N. Smirnov, I.A. Eliseyev, M.S. Dunaevskiy, E.V. Gushchina, K.A. Bokai, J. Pezoldt. Semiconductors **52**, *14*, 1882 (2018).

[8] T.M.G. Mohiuddin, A. Lombardo, R.R. Nair, A. Bonetti, G. Savini, R. Jalil, N. Bonini, D.M. Basko, C. Galiotis, N. Marzari, K.S. Novoselov, A.K. Geim, A.C. Ferrari. Phys. Rev. B **79**, *20*, 205433 (2009).

[9] I.A. Eliseyev, V.Yu. Davydov, A.N. Smirnov, M.O. Nestoklon, P.A. Dementev, S.P. Lebedev, A.A. Lebedev, A.V. Zubov, S. Mathew, J. Pezoldt, K.A. Bokai, D.Yu. Usachov. Semiconductors **53**, *14*, 1904 (2019).

[10] E.H. Martins Ferreira, M.V.O. Moutinho, F. Stavale, M.M. Lucchese, R.B. Capaz, C.A. Achete, A. Jorio. Phys. Rev. B **82**, 125429 (2010).

Translated by I.Mazurov